Advances in Concrete Construction, *Vol. 10, No. 3* (*2020*) *247-256*
DOI: https://doi.org/10.12989/acc.2020.10.3.247

Prediction of mechanical properties of limestone concrete after high temperature exposure with artificial neural networks

Urška Blumauer*[1], Tomaž Hozjan[1a] and Gregor Trtnik[2b]

[1]*Faculty of Civil and Geodetic Engineering, University of Ljubljana, Jamova 2, SI-1115 Ljubljana, Slovenia*
[2]*Building Materials Institute, IGMAT d.d., Polje 351c, SI-1000 Ljubljana, Slovenia*

(*Received February 20, 2020, Revised August 10, 2020, Accepted August 13, 2020*)

Abstract. In this paper the possibility of using different regression models to predict the mechanical properties of limestone concrete after exposure to high temperatures, based on the results of non-destructive techniques, that could be easily used in-situ, is discussed. Extensive experimental work was carried out on limestone concrete mixtures, that differed in the water to cement (w/c) ratio, the type of cement and the quantity of superplasticizer added. After standard curing, the specimens were exposed to various high temperature levels, i.e., 200°C, 400°C, 600°C or 800°C. Before heating, the reference mechanical properties of the concrete were determined at ambient temperature. After the heating process, the specimens were cooled naturally to ambient temperature and tested using non-destructive techniques. Among the mechanical properties of the specimens after heating, known also as the residual mechanical properties, the residual modulus of elasticity, compressive and flexural strengths were determined. The results show that residual modulus of elasticity, compressive and flexural strengths can be reliably predicted using an artificial neural network approach based on ultrasonic pulse velocity, residual surface strength, some mixture parameters and maximal temperature reached in concrete during heating.

Keywords: residual mechanical properties; compressive strength; artificial neural network; non-destructive testing techniques; fire behavior; concrete

1. Introduction

Reinforced concrete (RC) structures are built on a large scale mainly because of their durability and affordability. During their lifetime, however, in addition to earthquakes, the outbreak of a fire represents a significant risk of collapse or major damage to such structures. When exposed to high temperatures, various mechanical, chemical and thermal changes occur in concrete elements that are non-stationary and non-linear, but which are interconnected (Arioz 2007). Additional stresses are induced due to temperature and pore pressure differences in the concrete microstructure. This leads to the formation of microcracks in the concrete matrix and finally to permanent failure of the RC structure (Ada *et al*. 2018). All these changes affect the strength of the RC structure during and after fire exposure to different extent. For example, the compressive strength of concrete after exposure to high temperatures is around 20% lower than compressive strength measured during the exposure (Hertz 2005). Therefore, the determination of the residual strength of structures after fire on the basis of known residual mechanical properties is of utmost importance (Hertz 2005). Experimental investigations have shown that the type of cement, the type and size of aggregate, the w/c ratio, the load level and the cooling regime are the most important parameters that influence the residual compressive strength of the concrete (dos Santos and Rodrigues 2016). Consequently, different types of concrete behave differently after fire exposure (Ma *et al*. 2015). Hereinafter the focus of the research is on normal and high strength limestone concrete and its residual mechanical properties measured after exposure to high temperatures. Numerous experimental researches were already conducted on this topic, some of them are presented in (Hertz 2005, Savva *et al*. 2005, Arioz 2009, Varona *et al*. 2020). But residual mechanical properties or thermal damage of concrete after exposure to high temperatures can also be evaluated with non-destructive techniques like presented in (Chaix *et al*. 2003, Payan *et al*. 2007, Park *et al*. 2014, Krzemien and Hager 2015, Park *et al*. 2015, Park and Yim 2016, Park and Yim 2017, Dolinar *et al*. 2019). Based on the results of non-destructive testing techniques and corresponding destructive ones that are used for determination of residual mechanical properties, various regression models with explicit relationships between these results have been proposed in the literature (Savva *et al*. 2005, Yaqub and Bailey 2016, Park and Yim 2017, Dolinar *et al*. 2019). Savva *et al*. (2005) proposed a relationship between the compressive strength and ultrasonic (US) pulse velocity of limestone concrete at ambient temperature. For fire-damaged concrete Park and Yim (2016) provided a relationship between the residual dynamic modulus of elasticity determined by the resonant frequency method and the residual compressive strength. Park and Yim (2017) proposed relations between the results of nonlinear US

*Corresponding author, Ph.D. Student
E-mail: urska.blumauer@fgg.uni-lj.si
[a]Associate Professor
[b]Assistant Professor

ISSN: 2287-5301 (Print), 2287-531X (Online)

methods and residual mechanical properties. Recently, Dolinar *et al*. (2019) proposed a relationship for estimating the residual compressive strength of limestone concrete based on the residual shear modulus measured by the resonant frequency method. Furthermore the relationships between temperature and residual compressive strength of concrete are presented in the literature (Aslani and Samali 2013, Yang *et al*. 2018, Varona *et al*. 2018), however for the post-fire assessment of the concrete these relationships are not convenient due to difficult determination of the maximal temperature reached during a fire exposure.

The artificial neural network approach (ANN) can be successfully applied to concrete research, especially for the prediction of compressive strength. Based on the measured US pulse velocity and some concrete mix components, the prediction of the compressive strength of young concrete at ambient temperature was performed with ANN by Trtnik *et al*. (2009). Shah *et al*. (2012) predicted the residual compressive strength of concrete under stressed state at ambient temperature based on the results of non-linear US measurements and the ANN approach. Based on experimental studies, Chan *et al*. (1998) predicted the strength loss of concrete under high temperature with ANN. The input parameters included information about cement type, coarse aggregate type, additive type, proportion of mixed cement, w/c ratio, surface/volume ratio, maximum temperature, heating rate and duration at maximum temperature (Chan *et al*. 1998). Recently Abbas *et al*. (2019) presented an ANN approach to predict the residual compressive strength of high strength concrete after exposure to high temperatures. The proposed approach was determined based on a large set of experimental data obtained from the literature, e.g., (Shah *et al*. 2012). The best fit for predicting the residual strength of concrete was achieved for concrete with siliceous aggregate and known aggregate to cement ratio, w/c ratio and temperature as input parameters for ANN approach (Abbas *et al*. 2019). Taking different types of aggregate into account, the coefficient of determination for predicting residual compressive strength with ANN decreased. Turkmen *et al*. (2017) used an ANN model to predict the residual compressive strength of pumice aggregate concrete, with the input parameters consisted of the pumice to aggregate ratio and the target temperature.

In this paper the possibility of using different regression and ANN models to predict the residual mechanical properties of limestone concrete after exposure to high temperatures based on the results of some known non-destructive testing techniques that can be simply used in-situ, is discussed. The paper is a logical extension and enhancement of the paper recently published by the authors (Dolinar *et al*. 2019) and is based on extended experimental work.

2. Experimental setup

2.1 Material and specimen preparation

Various concrete mixtures were produced with Portland cement of high (CEM I 52.5 R) or normal (CEM I 42.5 N) strength, tap water, superplasticizer and limestone aggregate with rounded grains of nominal maximum size 16 mm. The concrete mixtures M1 and M2 contained high-strength cement and superplasticizer and differed in the w/c ratio, which was 0.47 and 0.34, respectively. The concrete mixes M3 and M4 were produced with high-strength and normal-strength cement respectively, with a w/c ratio of 0.49. The M5 mixture was made with high-strength cement and a w/c ratio of 0.45. The detailed compositions of the tested mixtures are summarized in Table 1.

Table 1 Composition of concrete mixtures used in the study, in [kg]

Material	Type	M1	M2	M3	M4	M5
Cement	Cem I 52.5 R	360	360	360	-	360
	Cem I 42.5 N	-	-	-	360	-
Water	Tap	169	122	175	177	161
Superplasticizer	PCE	2.16	2.16	-	-	-
Limestone aggregate	0-4 mm			931		
	4-8 mm			280		
	8-16 mm			652		

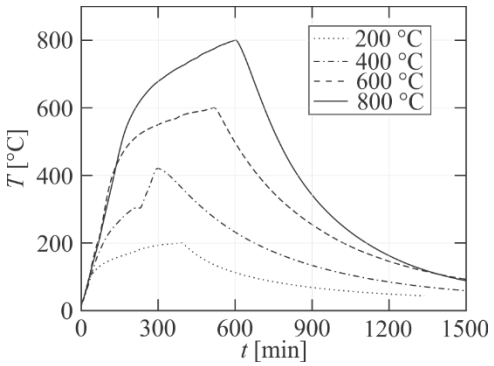

Fig. 1 Typical development of temperature T with time t inside concrete specimens

Prismatic and cubic specimens with the dimensions of 40×40×160 mm^3, and 100×100×100 mm^3 respectively, were produced. The specimens were cured in water for 28 days and finally air dried under standard laboratory conditions at 20±2°C and a relative humidity of ≥65%. All together 141 cubic and 101 prismatic specimens were produced.

2.2 Heating regime

The specimens were heated inside the electric furnace. During the process, the temperature development inside the furnace and the concrete specimens was carefully measured with previously calibrated high temperature resistant thermocouples installed 5 mm below the centre of the surface and in the centre of the cube.

Before heating, the concrete specimens of each mixture were divided into five groups. To obtain reference mechanical properties, the first group of specimens was tested immediately after the curing and drying process, i.e., before exposure to high temperatures. The other groups were exposed to high temperatures of 200°C, 400°C, 600°C or 800°C with a heating rate of about 3°C/min. After isothermal conditions had been established inside the

respective specimen, the specimens were naturally cooled to ambient temperature before they were experimentally investigated. Fig. 1 shows the typical development of temperature T with time t inside the specimens.

2.2 Testing procedures

Different non-destructive and destructive testing techniques were used to obtain different mechanical properties of concrete according to the relevant standards (EN 12504-4 2004, EN 12504-2 2002, ISO 1920-10 2010, EN 12390-3 2009, EN 12390-5 2009). Measurements with the US method were performed on all specimens, while the determination of the rebound number was performed on cubic specimens. The modulus of elasticity was then measured on prismatic specimens. Finally, compressive and bending tests were carried out on cubic and prismatic specimens, respectively.

In addition to the US and rebound number techniques, other non-destructive techniques were also performed. For the concrete mixtures M1 and M2 reference is made to (Dolinar *et al*. 2019), where comprehensive results of the non-destructive testing techniques are presented. As mentioned above, the aim of the paper is to investigate the prediction of residual mechanical properties of concrete after fire exposure based on the results of non-destructive testing techniques that could be used in-situ. Therefore, only the US pulse velocity and the residual surface strength are considered among all non-destructive techniques for the determination of the residual mechanical properties of limestone concrete. The experimental work was performed at IGMAT Building Materials Institute in Ljubljana, Slovenia.

Table 2 Normalized V_p measured on specimens of all concrete mixtures

T [°C]	M1	M2	M3	M4	M5
20	1.000	1.000	1.000	1.000	1.000
200	0.902	0.881	0.814	0.872	0.923
400	0.570	0.604	0.505	0.602	0.619
600	0.317	0.547	0.341	0.477	0.534
800	0.430	0.478	0.336	0.361	0.506

3. Experimental research

3.1 Experimental results

Fig. 2 shows the influence of the temperature T on the average values of the US pulse velocity, V_p, the residual surface strength, $f_{c,surf}$, the residual compressive strength, f_c, the residual flexural strength, f_{cf}, and the residual modulus of elasticity, E. The Tables 2-6 summarize the average measured results of the above mentioned quantities in normalized form.

The influence of the temperature T on V_p is shown in Fig. 2(a), while the normalized values for all concrete mixtures are summarized in Table 2. It can be seen that V_p of concrete specimens at ambient temperature equals approximately 4.0 km/s, which corresponds to good quality concrete (Yaqub and Bailey 2016). An increase in temperature to 200°C resulted in a decrease of V_p between 8% and 19% for the mixtures M5 and M3, respectively. The highest relative decrease of V_p (i.e., about 30%) is observed between 200°C and 400°C for all mixtures.

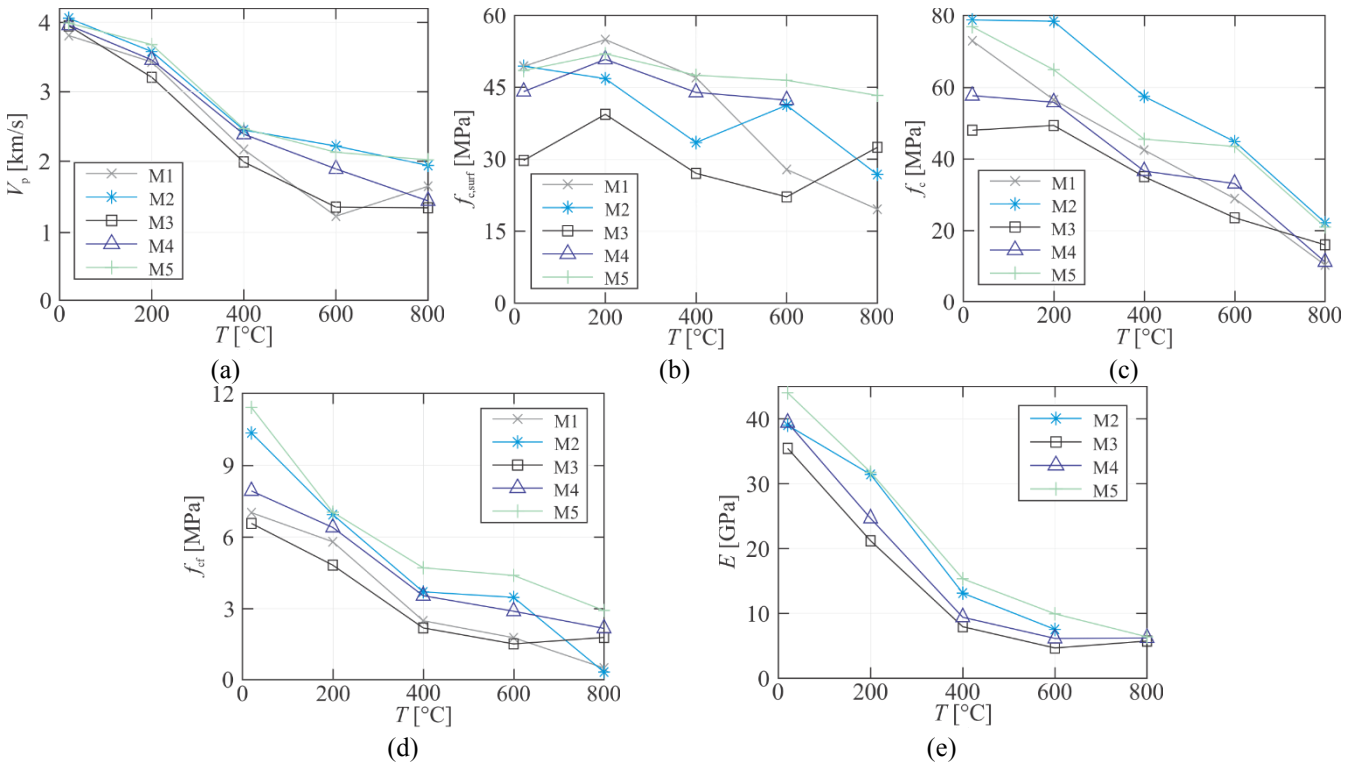

Fig. 2 Influence of temperature T on: (a) US pulse velocity, V_p, (b) residual surface strength, $f_{c,surf}$, (c) residual compressive strength, f_c, (d) residual flexural strength, f_{cf}, and (e) residual elastic modulus, E

Table 3 Normalized $f_{c,surf}$ determined on specimens for all concrete mixtures

T [°C]	M1	M2	M3	M4	M5
20	1.000	1.000	1.000	1.000	1.000
200	1.113	0.947	1.323	1.153	1.072
400	0.952	0.678	0.909	0.996	0.980
600	0.564	0.835	0.744	0.960	0.958
800	0.397	0.543	1.092	*	0.893

*Due to the extensive damage of the specimens after heating, determination of $f_{c,surf}$ was not possible.

Table 4 Normalized f_c determined on concrete cubes for all mixtures

T [°C]	M1	M2	M3	M4	M5
20	1.000	1.000	1.000	1.000	1.000
200	0.774	0.995	1.028	0.968	0.844
400	0.581	0.728	0.729	0.634	0.591
600	0.395	0.568	0.489	0.573	0.564
800	0.141	0.280	0.331	0.193	0.271

Table 5 Normalized f_{cf} determined on concrete prisms for all mixtures

T [°C]	M1	M2	M3	M4	M5
20	1.000	1.000	1.000	1.000	1.000
200	0.825	0.669	0.733	0.806	0.615
400	0.352	0.356	0.332	0.445	0.411
600	0.251	0.334	0.228	0.363	0.382
800	0.070	0.031	0.270	0.272	0.254

Table 6 Normalized E determined on concrete prisms for mixtures M2 to M5

T [°C]	M2	M3	M4	M5
20	1.000	1.000	1.000	1.000
200	0.805	0.598	0.625	0.722
400	0.336	0.224	0.238	0.348
600	0.193	0.131	0.156	0.225
800	*	0.162	0.157	0.145

*Due to the extensive damage of the specimens after heating, determination of E was not possible.

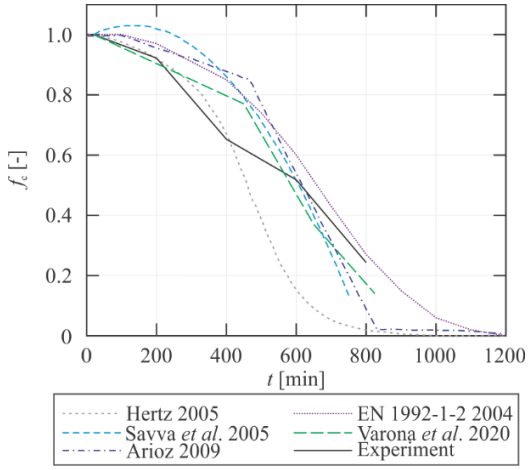

Fig. 3 The values of normalized residual compressive strength f_c of limestone concrete obtained from the present experiment and literature

The influence of the temperature T on $f_{c,surf}$ is shown in Fig. 2(b) and the normalized values are shown in Table 3. At 200°C the results show an increase of $f_{c,surf}$ between 7% (M5) and 32% (M3). The highest relative decrease for mixtures M2 to M5 is observed between 200°C and 400°C (between 9% for mixture M5 and 41% for mixture M3), while for mixture M1 the highest relative decrease is observed between the temperature 400°C and 600°C (39%).

The residual compressive strength, f_c, and the normalized values of f_c as a function of temperature are shown in Fig. 2(c) and Table 4, respectively. As expected, the composition of concrete mixtures has a major influence on f_c. In all cases, a temperature rise resulted in a steep and almost linear drop of f_c. It can be observed that for each mixture, the highest relative decrease of f_c is about 30 %. However, this reduction took place at different temperature levels depending on the composition of the concrete.

The residual flexural strength, f_{cf}, and the normalized values of f_{cf} as a function of temperature T are shown in Fig. 2(d) and Table 5, respectively. As expected, f_{cf} decreases with increase of temperature T. However, the decrease of f_{cf} is more pronounced in the temperature range between 200°C and 400°C, which corresponds very well with the temperature at the formation of conspicuous cracks on the surface of the specimens (Dolinar *et al.* 2019).

The residual modulus of elasticity, E, was measured on concrete prisms of mixtures M2 to M5, and its variation with temperature and normalized values are shown in Fig. 2(e) and Table 6, respectively. A strong decline of the E with increase of temperature T is clearly visible in the figure. The highest relative decrease of about 40% is observed between 20°C and 200°C and between 200°C and 400°C for the mixture M3 and for the mixtures M2, M4 and M5, respectively.

3.2 Comparison to experimental results obtained from the literature

Among all residual mechanical properties of concrete, the residual compressive strength is the most investigated one. After exposure to high temperatures limestone concrete was also investigated by Hertz (2005), Savva *et al.* (2005), Arioz (2009) and Varona *et al.* (2020). Fig. 3 presents average experimental residual compressive strength in comparison with aforementioned authors. Additionally, the compressive strength of limestone concrete during exposure to high temperatures according to the standard EN 1992-1-2 (2004) is given in Fig. 3.

A great dispersion of the curves is observed in the Fig. 3, however all residual compressive strengths of limestone concrete determined after exposure to high temperature are from 600°C onward lower that compressive strength during the exposure to high temperature according to the standard EN 1992-1-2 (2004).

4. Regression models with explicit relationships

4.1 Introduction

Table 7 Regression models with explicit relationships for prediction of f_c

	Explicit relationship	R^2	RMSE
(a)	$f_c = 16.06\ V_p + 1.234$	0.7101	10.05
(b)	$f_c = 17.64\ e^{0.02201\ f_{c,surf}}$	0.3234	15.36
(c)	$f_c = 9.759 - 6.4\ V_p + 0.9336\ f_{c,surf} + 0.6534\ V_p^2 + 0.4941\ V_p f_{c,surf} - 0.02663\ f_{c,surf}^2$	0.8146	8.21

Table 8 Regression models with explicit relationships for prediction of f_{cf}

	Explicit relationship	R^2	RMSE
(a)	$f_{cf} = 0.7702\ V_p^{1.766}$	0.8016	1.27
(b)	$f_{cf} = 0.0005178\ f_{c,surf}^2 + 0.1076\ f_{c,surf} - 0.5492$	0.3974	2.22
(c)	$f_{cf} = 0.4476 - 1.521\ V_p + 0.07495\ f_{c,surf} + 0.3696\ V_p^2$	0.8651	1.07

Regression analysis is a statistical process in which the influence of one or more independent variables is examined against a dependent one. The performance of a regression model is normally evaluated with the coefficient of determination, R^2, and the root mean square error (RMSE). Explicit relationships between the results of non-destructive techniques and residual mechanical properties f_c, f_{cf} or E are presented in Sections 4.2, 4.3 and 4.5, respectively. In the first case (a), the relationship between the selected residual mechanical property and the US pulse velocity, V_p, is proposed. The following case (b) suggests the relationship between the residual mechanical property and the residual surface strength, $f_{c,surf}$, and the last case, (c), suggests the relationship between the residual mechanical property and V_p, and $f_{c,surf}$. Detailed regression models using explicit relationships to determine the residual mechanical properties of limestone concrete are presented by the authors in (Dolinar *et al*. 2019), but on a smaller data set.

4.2 Residual compressive strength

Table 7 summarizes proposed regression models with explicit relationships for the prediction of f_c and corresponding R^2 and RMSE for all three cases. The best prediction of f_c is achieved in case (c) where V_p and $f_{c,surf}$ are taken into account. In this case the R^2 is 0.8146 and the corresponding RMSE is equal to 8.21. If V_p (case a) is taken into account alone, the prediction of f_c is slightly worse, while taking $f_{c,surf}$ as the only input parameter for the prediction of f_c turns out to be inappropriate.

4.3 Residual flexural strength

Table 8 summarizes proposed regression models with explicit relationships for the prediction of f_{cf} with corresponding R^2 and RMSE for all three cases. Similar to the prediction of f_c, the best prediction of f_{cf} is achieved in case (c), where the corresponding R^2, and RMSE are 0.8651 and 1.07, respectively. With the consideration of V_p alone (case a) the prediction of f_{cf} is comparable, while the consideration of $f_{c,surf}$ (case b) as the only input parameter for the prediction of f_{cf}, similar to the prediction of f_c, is once more recognized as unsuitable.

Table 9 Regression models with explicit relationships for prediction of E

	Explicit relationship	R^2	RMSE
(a)	$E = 4.01\ V_p^2 - 8.44\ V_p + 8.32$	0.9421	3.36
(b)	$E = 4.25\ e^{0.0368\ f_{c,surf}}$	0.2307	12.16
(c)	$E = 6.865 - 12.26\ V_p + 0.3597\ f_{c,surf} + 4.267\ V_p^2$	0.9449	3.34

4.4 Residual elastic modulus

Table 9 summarizes proposed regression models with explicit relationships for the prediction of E with corresponding R^2 and RMSE. The best prediction of the residual mechanical property is again achieved in case (c). The E value could just as well be predicted on the basis of known V_p alone, whereas a prediction based on measured $f_{c,surf}$ (case b) is not suitable.

5. Regression models using artificial neural networks

5.1 Artificial neural networks

The basic idea and motivation for the development of ANN comes from the structure and natural processes that take place in the biological nervous system, since they are similar in many aspects to functioning neural networks. The ANN approach is a massively parallel distributed processor consisting of simple processing units that have a natural tendency to store experimental knowledge and make it available for use (Haykin 2009). Therefore, ANNs have excellent performance, accuracy and versatility and are known as universal proximity systems. It has been shown that a standard multi-layer feed-forward neural network is capable of approximating any measurable function and that there are no theoretical limitations to its success (Hornik *et al*. 1989). A detailed description of ANN is available elsewhere in the literature, for example (Chan *et al*. 1998, Shah *et al*. 2012, Abbas *et al*. 2019, Haykin 2009).

In the present study, different forms of a typical multi-layer feed-forward ANN were tested with a different number of hidden layers and a different number of neurons in each layer. Since the amount of experimental results is small, a maximum of two hidden layers is sufficient for the prediction of selected residual mechanical property as proposed in (Vakharia and Gujar 2019). In addition, the selection of a high number of neurons in hidden layers can lead to overtraining, as described in (Gupta *et al*. 2019). The neurons in the hidden layer are characterized by a hyperbolic tangential sigmoid transfer function described in (Yonaba *et al*. 2010). The input and output layers consist of known data, while the weights in the hidden layer(s) were determined during the training process. The set of experimental results was divided into input and output data, called input-output pairs. A cross-validation technique was used to improve the generalization capacity and avoid overfitting. Therefore, the input-output pairs were randomly divided into five different folds, and each input-output pair

was used once in the test set. This method was previously successfully used by Vakharia and Gujar (2019) to predict the compressive strength and composition of Portland cement. Next, five folds were divided into training and testing sets. The training set included approximately 80 % of input-output pairs, that is four folds, which were used to determine the connection weights and thresholds of neurons in the hidden layer(s). Levenberg-Marquardt backpropagation algorithm and Bayesian Regularization were used for this purpose (Hagan *et al*. 2014). The latter is often used to improve the generalization capacity of ANN. The performance of the neural networks was tested on the testing set that included the remaining fold (i.e., 20% of input-output pairs). The accuracy of the prediction of residual mechanical properties was estimated with R^2 and RMSE. The analyzes were performed with the Matlab computer programming environment (Matlab 1999).

5.2 Analysis

In the input layer of ANNs different non-destructive test results like V_p and $f_{c,surf}$ as well as w/c ratio or temperature T were used. The output layer included f_c (presented in Section 5.3), f_{cf} (presented in Section 5.4) or E (presented in Section 5.5).

In the first case (a) the selected residual mechanical property was predicted based on V_p alone. The following case (b) predicted the residual mechanical property based on V_p, and $f_{c,surf}$. Next, the prediction was based on the results of all non-destructive techniques and the w/c ratio (c) or T (d). Finally, in case (e) all known data were used to predict the selected residual mechanical property (V_p, $f_{c,surf}$, w/c ratio and T). The influence of input parameters on the accuracy of learning performance of ANN was thus investigated.

For the two selected training algorithms, the difference between the average maximum R^2 determined with Levenberg-Marquardt and Bayesian Regularization was at most 2% when predicting f_{cf}. The results presented below were obtained with the Bayesian Regularization training algorithm. Appendix A, Tables A1-A3, show the accuracy of learning performance assessed with the average R^2 for the five-fold cross-validation method. The highest average value of R^2 for each selected case is marked bold in the Tables A1-A3. The columns in the Tables A1-A3, represent different cases depending on the number of input parameters selected in the input layer of the ANN, and the rows represent different geometries of ANN (ANN's geometry), where each digit represents the number of neurons in each hidden layer.

5.3 Prediction of residual compressive strength

As can be seen from the Table A1, that the highest R^2 (i.e., 0.9429) is reached in the case where all input parameters are considered (case e). This was achieved with the ANN geometry of only one hidden layer and four neurons. Nevertheless, a similar accuracy of the ANNs in case (e) is also achieved for the other examined geometries. In cases (c) and (d), where the w/c ratio and the T were considered separately as input parameters, the maximum R^2 was about 10% lower than in case (e).

Fig. A1 in Appendix A shows the relationships between the predicted and measured results for all five folds for the ANN with the highest average R^2. The determination of the RMSE for each fold was presented to estimate the accuracy of the ANN used, since a smaller error between predicted and measured results indicates better accuracy. The minimum (3.128) and maximum (5.28) RMSE was reached in the 4th and 5th fold, respectively. For comparison, the RMSE values for the ANN with one neuron in each hidden layer for case (e) were determined. Here the R^2 value is the lowest for case (e), i.e., 0.9062. The RMSE values for folds one to five are 6.297, 6.419, 5.607, 3.663 and 6.427, respectively. For comparison, Vakharia and Gujar (2019) achieved the RMSE value around 8 for the prediction of f_c of high-performance concrete at ambient temperature using ANN and ten-fold cross-validation method.

5.4 Prediction of residual flexural strength

Again, relationships for the prediction of the f_{cf} were determined based on different ANN geometries and different input parameters. The average R^2 values for the five-fold cross-validation method are shown in Table A2. For the best prediction of the f_{cf} it is important to consider V_p, $f_{c,surf}$ and w/c ratio. In this case, the R^2 is 0.8739 and the corresponding minimum RMSE was 0.6402 and the maximum RMSE was 1.231. Interestingly, while considering V_p and $f_{c,surf}$ as input parameters (case b), the decrease of value of R^2 was not significant. Hence from a practical point of view, considering only V_p and $f_{c,surf}$ would result in a good prediction of f_{cf}.

5.5 Prediction of residual elastic modulus

Also for the prediction of the E relationships with different ANN geometries and different input parameters were determined. The best prediction of the E is observed when all considered input parameters are taken into account. In this case, the average value of R^2 was 0.9602 and the corresponding minimum and maximum RMSE were 1.509 and 3.944, respectively. Taking into account V_p and $f_{c,surf}$ obtained with non-destructive techniques, and the w/c ratio (case c) as input parameters for ANN, the maximum R^2 is comparable to case (e) when all input parameters are considered. It is also noted that the average R^2 is high, even in the case of the simplest neural network geometry, and even if V_p is considered as the only input parameter (case a).

6. Discussion

As mentioned above, the prediction of residual mechanical properties on the basis of results of non-destructive testing techniques, w/c ratio and temperature is investigated. The results indicate that the prediction of f_{cf} and E could be based on V_p, $f_{c,surf}$ and the w/c ratio. In practice, the latest information could be obtained from the design project of an investigated building. However, as observed in Section 5.3, information about the maximum

temperature of the concrete member reached during a fire exposure is of great importance for the accurate prediction of f_c. During the experimental investigation, such temperatures can be measured with pre-installed thermocouples, whereas this is no longer possible on the building after the fire. As mentioned in (Molkens *et al*. 2017), the assessment of post-fire load-bearing capacity needs to rely on rigorous methods. It is possible to reproduce the possible fire scenario models based on the results of various in-situ measurements after a fire. On the basis of such models the fire development and the mechanical response of the structure after a fire could be estimated. In (Molkens *et al*. 2017) a post-fire assessment of an apartment after a fire was done. For this purpose, the prediction of the maximum temperatures in the fire most exposed concrete slab was carried out on the basis of the estimation of the fire duration obtained by the firefighters and using the software OZone (Cadorin and Franssen 2003) for predicting the gas temperature. The measured residual vertical deflection of the concrete slab after a fire was taken into account in the finite element method for modeling the structural response. Within the iteration process different gas temperatures were used as input parameters for the finite element model until the numerical and measured residual vertical deflection coincided. In similar way, presented ANN for the prediction of f_c could be used, based on the numerically determined maximum temperature reached in the concrete member obtained from a possible fire scenario.

7. Conclusions

The focus of the present work was on the use of available data from non-destructive methods that can easily be applied in-situ, and on some known mix parameters of concrete to predict the residual mechanical properties of concrete after a fire. This information is of utmost importance for estimating the residual load-bearing capacity of concrete structures after a fire. For this purpose, extensive experimental work was carried out on five different concrete mixtures with limestone aggregate. The ability of regression models with explicit relationships and ANN approach to determine residual mechanical properties has been investigated. In the case of predicting f_c the highest value of R^2 (0.9429) was reached with ANN where the input parameters consisted of V_p, $f_{c,surf}$, w/c ratio and T. This result agrees well with the research work of Abbas *et al*. (2019) on a larger data set where the highest value of R^2 for predicting the residual compressive strength of high-strength concrete after exposure to high temperature and known aggregate to cement ratio, w/c ratio and temperature for siliceous aggregate was 0.958. Similarly, the best prediction of f_{cf} was obtained using an ANN approach where the input parameters consisted of V_p, $f_{c,surf}$ and the w/c ratio. In this case, however, a very similar R^2 was achieved using a regression model with explicit relationship, considering V_p and $f_{c,surf}$ as input parameters. As for the prediction of f_{cf}, the best prediction of E was achieved using ANN approach, while a similarly good prediction was achieved with explicit relationship. The ANN approach considered all input parameters, while for the explicit relationship only results of V_p, and $f_{c,surf}$ were considered.

The results show that the application of this ANN approach is suitable for predicting the residual compressive strength of concrete after a fire. However, in the case of the prediction of residual flexural strength and modulus of elasticity, the accuracy of the results obtained with regression models using explicit relationships is comparable. Therefore, both regression models can be used successfully in practice if they are applied properly.

Acknowledgments

The work of U. Blumauer was financially supported by Slovenian Research Agency with decision No. 802-7/2016-215. The work of T. Hozjan and G. Trtnik was also supported by the Slovenian Research Agency through the research core funding No. P2-0260. The support is gratefully acknowledged.

References

Abbas, H., Al-Salloum, Y.A., Elsanadedy, H.M. and Almusallam, T.H. (2019), "ANN models for prediction of residual strength of HSC after exposure to elevated temperatures", *Fire Saf. J.*, **106**, 13-28. https://doi.org/10.1016/j.firesaf.2019.03.011.

Ada, M., Sevim, B., Yuzer, N. and Ayvaz, Y. (2018), "Assessment of damages on a RC building after a big fire", *Adv. Concrete Constr.*, **6**(2), 177-197. https://doi.org/10.12989/acc.2018.6.2.177.

Arioz, O. (2007), "Effects of elevated temperatures on properties of concrete", *Fire. Saf. J.*, **42**(8), 516-522. https://doi.org/10.1016/j.firesaf.2007.01.003.

Arioz, O. (2009), "Retained properties of concrete exposed to high temperatures: Size effect", *Fire Mater.*, **33**, 211-222. https://doi.org/10.1002/fam.996.

Aslani, F. and Samali, B. (2013), "Predicting the bond between concrete and reinforcing steel at elevated temperatures", *Struct. Eng. Mech.*, **48**(5), 643-660. http://dx.doi.org/10.12989/sem.2013.48.5.643.

Cadorin, J.F. and Franssen, J.M. (2003), "A tool to design steel elements submitted to compartment fires - OZone V2. Part 1: pre- and post-flashover compartment fire model", *Fire Saf. J.*, **38**, 395-427. https://doi.org/10.1016/S0379-7112(03)00014-6.

Chaix, J.F., Garnier, V. and Corneloup, G. (2003), "Concrete damage evolution analysis by backscattered ultrasonic waves", *NDT E Int.*, **36**(7), 461-469. https://doi.org/10.1016/S0963-8695(03)00066-5.

Chan, Y.N., Jin, P., Anson, M. and Wang, J.S. (1998), "Fire resistance of concrete: prediction using artificial neural networks", *Mag. Concrete Res.*, **50**(4), 353-358. https://doi.org/10.1680/macr.1998.50.4.353.

Dolinar, U., Trtnik, G., Turk, G. and Hozjan, T. (2019), "The feasibility of estimation of mechanical properties of limestone concrete after fire using nondestructive methods", *Constr. Build. Mater.*, **228**, 116786. https://doi.org/10.1016/j.conbuildmat.2019.116786.

dos Santos, C.C. and Rodrigues, J.P.C. (2016), "Calcareous and granite aggregate concretes after fire", *J. Build. Eng.*, **8**, 231-242. https://doi.org/10.1016/j.jobe.2016.09.009.

EN 12390-3:2009, Testing Hardened Concrete - Part 3: Compressive Strength of Test Specimens.

EN 12390-5:2009, Testing Hardened Concrete - Part 5: Flexural Strength of Test Specimens.

EN 12504-2:2002, Testing Concrete in Structures - Part 2: Non-Destructive Testing - Determination of Rebound Number.

EN 12504-4: 2004, Testing Concrete - Part 4: Determination of Ultrasonic Pulse Velocity.

EN 1992-1-2:2004, Eurocode 2: Design of Concrete Structures - Part 1-2: General Rules - Structural Fire Design.

Gupta, T., Patel, K.A., Siddique, S., Sharma, R.K. and Chaudhary, S. (2019), "Prediction of mechanical properties of rubberised concrete exposed to elevated temperature using ANN", *Measure.*, **147**, 106870. https://doi.org/10.1016/j.measurement.2019.106870.

Hagan, M.T., Demuth, H.B., Beale, M.H. and De Jesus, O. (2014), *Neural Network Design*, 2nd Edition, Self Published.

Haykin, S. (2009), *Neural Networks and Learning Machines*, Pearson Education, Inc., Upper Saddle River, New Jersy.

Hertz, K.D. (2005), "Concrete strength for fire safety design", *Mag. Concrete Res.*, **57**(8), 445-453. https://doi.org/10.1680/macr.2005.57.8.445.

Hornik, K., Stinchcombe, M. and White, H. (1989), "Multilayer feedforward networks are universal approximators", *Neur. Network.*, **2**(5), 359-366. https://doi.org/10.1016/0893-6080(89)90020-8.

ISO 1920-10:2010, Testing of Concrete - Part 10: Determination of Static Modulus of Elasticity in Compression.

Krzemien, K. and Hager, I. (2015), "Post-fire assessment of mechanical properties of concrete with the use of the impact-echo method", *Constr. Build. Mater.*, **96**, 155-163. https://doi.org/10.1016/j.conbuildmat.2015.08.007.

Ma, Q.M., Guo, R.X., Zhao, Z.M., Lin, Z.W. and He, K.C. (2015), "Mechanical properties of concrete at high temperature - a review", *Constr. Build. Mater.*, **93**, 371-383. http://dx.doi.org/10.1016/j.conbuildmat.2015.05.131.

Matlab (1999) The Language of Technical Computing, The Mathworks Inc.

Molkens, T., Van Coile, R. and Gernay, T. (2017), "Assessment of damage and residual load bearing capacity of concrete slab after fire: Applied reliability-based methodology", *Eng. Struct.*, **150**, 969-985. http://dx.doi.org/10.1016/j.engstruct.2017.07.078.

Park, G.K. and Yim, H.J. (2017), "Evaluation of fire-damaged concrete: An experimental analysis based on destructive and nondestructive methods", *Int. J. Concrete Struct. Mater.*, **11**(3), 447-457. https://doi.org/10.1007/s40069-017-0211-x.

Park, S.J. and Yim, H.J. (2016), "Evaluation of residual mechanical properties of concrete after exposure to high temperatures using impact resonance method", *Constr. Build. Mater.*, **129**, 89-97. https://doi.org/10.1016/j.conbuildmat.2016.10.116.

Park, S.J., Park, G.K., Yim, H.J. and Kwak, H.G. (2015), "Evaluation of residual tensile strength of fire-damaged concrete using a non-linear resonance vibration method", *Mag. Concrete Res.*, **67**(5), 235-246. https://doi.org/10.1680/macr.14.00259.

Park, S.J., Yim, H.J. and Kwak, H.G. (2014), "Nonlinear resonance vibration method to estimate the damage level on heat-exposed concrete", *Fire Saf. J.*, **69**, 36-42. https://doi.org/10.1016/j.firesaf.2014.07.003.

Payan, C., Garnier, V., Moysan, J. and Johnson, P.A. (2007), "Applying nonlinear resonant ultrasound spectroscopy to improving thermal damage assessment in concrete", *J. Acoust. Soc. Am.*, **121**(4), EL125-EL130. https://doi.org/10.1121/1.2710745.

Savva, A., Manita, P. and Sideris, K.K. (2005), "Influence of elevated temperatures on the mechanical properties of blended cement concretes prepared with limestone and siliceous aggregates", *Cement Concrete Compos.*, **27**(2), 239-248. https://doi.org/10.1016/j.cemconcomp.2004.02.013.

Shah, A.A., Alsayed, S.H., Abbas, H. and Al-Salloum, Y.A. (2012), "Predicting residual strength of non-linear ultrasonically evaluated damaged concrete using artificial neural network", *Constr. Build. Mater.*, **29**, 42-50. https://doi.org/10.1016/j.conbuildmat.2011.10.038.

Trtnik, G., Kavčič, F. and Turk, G. (2009), "Prediction of concrete strength using ultrasonic pulse velocity and artificial neural networks", *Ultrasonics*, **49**(1), 53-60. https://doi.org/10.1016/j.ultras.2008.05.001.

Turkmen, I., Bingol, A.F., Tortum, A., Demirboga, R. and Gul, R. (2017), "Properties of pumice aggregate concretes at elevated temperatures and comparison with ANN models", *Fire Mater.*, **41**, 142-153. https://doi.org/10.1002/fam.2374.

Vakharia, V. and Gujar, R. (2019), "Prediction of compressive strength and portland cement composition using cross-validation and feature ranking techniques", *Constr. Build. Mater.*, **225**, 292-301. https://doi.org/10.1016/j.conbuildmat.2019.07.224.

Varona, F.B., Baeza, F.J., Bru, D. and Ivorra, S. (2018), "Evolution of the bond strength between reinforcing steel and fibre reinforced concrete after high temperature exposure", *Constr. Build. Mater.*, **176**, 359-370. https://doi.org/10.1016/j.conbuildmat.2018.05.065.

Varona, F.B., Baeza, F.J., Bru, D. and Ivorra, S. (2020), "Non-linear multivariable model for predicting the steel to concrete bond after high temperature exposure", *Constr. Build. Mater.*, **249**, 118713. https://doi.org/10.1016/j.conbuildmat.2020.118713.

Yang, O., Zhang, B., Yan, G. and Chen, J. (2018), "Bond performance between slightly corroded steel bar and concrete after exposure to high temperature", *J. Struct. Eng.*, **144**(11), 04018209. https://doi.org/10.1061/(ASCE)ST.1943-541X.0002217.

Yaqub, M. and Bailey, C.G. (2016), "Non-destructive evaluation of residual compressive strength of post-heated reinforced concrete columns", *Constr. Build. Mater.*, **120**, 482-493. https://doi.org/10.1016/j.conbuildmat.2016.05.022.

Yonaba, H., Anctil, F. and Fortin, V. (2010), "Comparing sigmoid transfer functions for neural network multistep ahead streamflow forecasting", *J. Hydrol. Eng.*, **15**(4), 275-283. https://doi.org/10.1061/(ASCE)HE.1943-5584.0000188.

CC

Appendix A.

Table A1 Average values of R^2 obtained from different ANN's geometry trained with Bayesian Regularization, and various input parameters for the prediction of f_c

ANN's geometry	(a)	(b)	(c)	(d)	(e)
0	0.7118	0.7237	0.7632	0.8072	0.9114
1	0.7145	0.7481	0.8065	0.7993	0.9129
2	0.7112	0.7825	0.8349	0.8157	0.9247
3	0.7106	0.7506	0.8384	0.8215	0.9342
4	0.7106	0.7593	0.8379	0.8222	**0.9429**
5	0.7114	0.7871	0.8340	0.8228	0.9329
1-1	0.7135	0.7471	0.8045	0.7955	0.9062
1-2	0.7114	0.7466	0.8057	0.7987	0.9123
1-3	0.7123	0.7474	0.8057	0.8011	0.9098
1-4	0.7096	0.7486	0.8066	0.8007	0.9109
2-1	0.7153	0.7533	0.8480	0.8157	0.9254
2-2	**0.7154**	0.7540	0.8482	0.8482	0.9262
2-3	0.7125	0.7636	0.8471	0.8227	0.9325
2-4	0.7101	0.7553	0.8470	0.8228	0.9334
3-1	0.7115	0.7817	0.8455	0.8482	0.9304
3-2	0.7119	**0.7903**	**0.8514**	**0.8490**	0.9340
3-3	0.7106	0.7901	0.8470	0.8479	0.9320
3-4	0.7099	0.7902	0.8460	0.8423	0.9321
4-1	0.7126	0.7874	0.8450	0.8420	0.9331
4-2	0.7096	0.7622	0.8480	0.8451	0.9323
4-3	0.7094	0.7749	0.8396	0.8480	0.9308
4-4	0.7105	0.7890	0.8439	0.8468	0.9290

Table A2 Average values of R^2 obtained from different ANN's geometry trained with Bayesian Regularization, and various input parameters for the prediction of f_{cf}

ANN's geometry	(a)	(b)	(c)	(d)	(e)
0	0.7949	0.8171	0.8274	0.8120	0.8246
1	0.8065	0.8380	0.8411	0.8083	0.8478
2	0.8087	0.8518	0.8601	0.8412	0.8569
3	0.8042	0.8467	0.8659	0.8402	0.8627
4	0.8059	0.8509	0.8635	0.8483	0.8672
5	0.8087	0.8503	0.8654	0.8526	0.8667
1-1	**0.8127**	0.8523	0.8524	0.8336	0.8608
1-2	0.8096	0.8459	0.8620	0.8405	0.8490
1-3	0.8036	0.8471	0.8567	0.8475	0.8533
1-4	0.8104	0.8495	0.8643	0.8397	0.8612
2-1	0.8083	0.8414	0.8651	0.8425	0.8572
2-2	0.8125	0.8548	0.8697	0.8512	0.8637
2-3	0.8051	0.8562	0.8641	**0.8537**	0.8610
2-4	0.8122	**0.8576**	0.8710	0.8441	**0.8692**
3-1	0.8066	0.8549	0.8654	0.8513	0.8687
3-2	0.8116	0.8531	0.8692	0.8457	0.8643
3-3	0.8097	0.8544	**0.8739**	0.8461	0.8644
3-4	0.8105	0.8508	0.8682	0.8518	0.8634
4-1	0.8109	0.8547	0.8682	0.8448	0.8584
4-2	0.8110	0.8542	0.8651	0.8502	0.8619
4-3	0.8071	0.8560	0.8684	0.8481	0.8651
4-4	0.8100	0.8488	0.8699	0.8450	0.8609

Table A3 Average values of R^2 obtained from different ANN's geometry trained with Bayesian Regularization, and various input parameters for the prediction of E

ANN's geometry	(a)	(b)	(c)	(d)	(e)
0	0.8741	0.8827	0.8815	0.9067	0.9074
1	0.9424	0.9412	0.9402	0.9539	0.9552
2	0.9425	0.9418	0.9383	0.9540	0.9537
3	**0.9449**	0.9417	0.9358	0.9543	0.9536
4	0.9427	0.9412	0.9393	0.9550	0.9592
5	0.9427	0.9412	0.9387	0.9547	0.9583
1-1	0.9416	0.9403	0.9402	0.9518	0.9552
1-2	0.9424	0.9405	0.9408	0.9515	0.9542
1-3	0.9422	0.9424	0.9406	0.9521	0.9547
1-4	0.9427	0.9414	0.9415	0.9523	0.9557
2-1	0.9436	0.9443	0.9421	0.9551	**0.9602**
2-2	0.9391	0.9418	**0.9422**	0.9549	0.9555
2-3	0.9435	0.9436	0.9398	0.9535	0.9512
2-4	0.9427	0.9416	0.9337	0.9531	0.9534
3-1	0.9433	0.9439	0.9416	0.9541	0.9529
3-2	0.9420	**0.9444**	0.9367	0.9550	0.9565
3-3	0.9425	0.9441	0.9385	0.9552	0.9526
3-4	0.9420	0.9431	0.9404	0.9542	0.9570
4-1	0.9428	0.9428	0.9394	0.9541	0.9549
4-2	0.9427	0.9438	0.9371	0.9545	0.9556
4-3	0.9422	0.9442	0.9332	**0.9554**	0.9568
4-4	0.9427	0.9443	0.9360	0.9546	0.9588

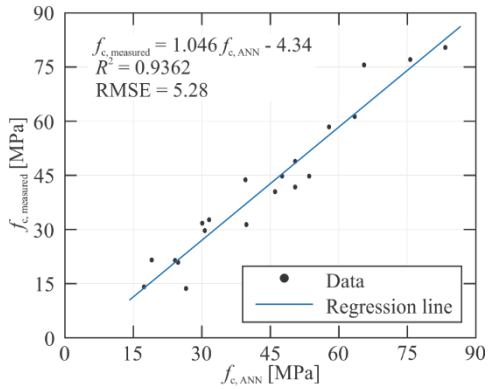

(a)

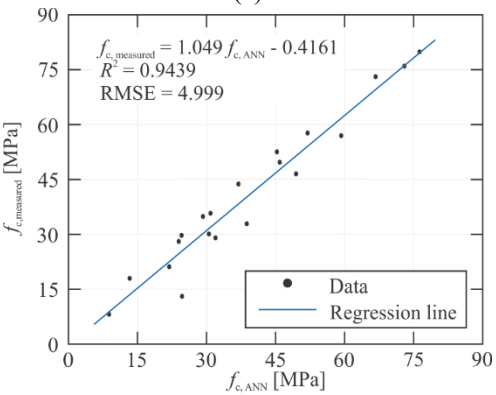

(b)

Fig. A1 Regression lines between the best prediction of f_c with ANN and measured f_c using five-fold cross-validation method and Bayesian Regularization training algorithm: (a) first fold, (b) second fold, (c) third fold, (d) fourth fold, and (e) fifth fold

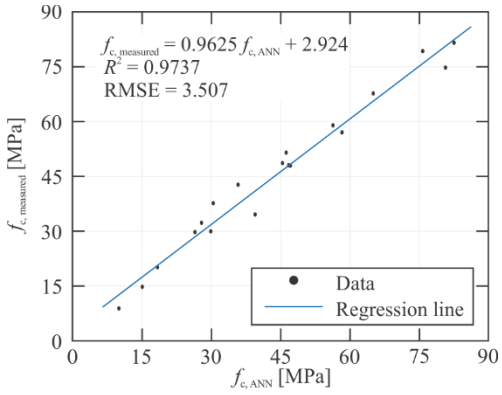

(c)

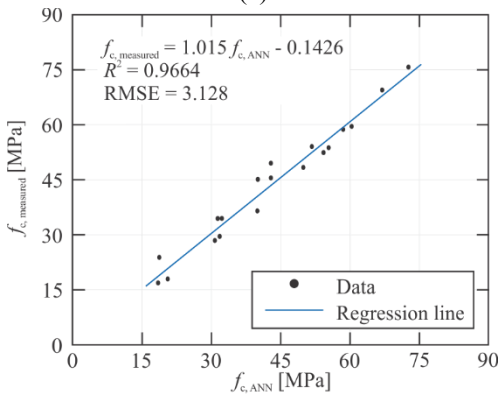

(d)

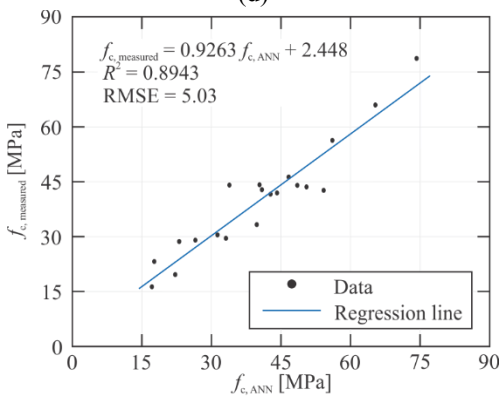

(e)

Fig. A1 Continued